Identification of complex crack damage for honeycomb sandwich plate using wavelet analysis and neural networks

2003 Smart Mater. Struct. 12 661

(http://iopscience.iop.org/0964-1726/12/5/301)

INSTITUTE OF PHYSICS PUBLISHING SMART MATERIALS AND STRUCTURES
Smart Mater. Struct. **12** (2003) 661–671 PII: S0964-1726(03)64809-3

Identification of complex crack damage for honeycomb sandwich plate using wavelet analysis and neural networks

L H Yam[1,3], Y J Yan[1,2], L Cheng[1] and J S Jiang[2]

[1] Department of Mechanical Engineering, The Hong Kong Polytechnic University, Hung Hom, Kowloon, Hong Kong SAR, People's Republic of China
[2] Institute of Vibration Engineering, Northwestern Polytechnic University, Xi'an 710072, People's Republic of China

E-mail: mmlhyam@polyu.edu.hk

Received 10 July 2002, in final form 19 May 2003
Published 1 August 2003
Online at stacks.iop.org/SMS/12/661

Abstract
In this study, crack damage detection for a honeycomb sandwich plate is studied using the energy spectrum of dynamic response decomposed by wavelet transform and the artificial neural network (NN). The results show that taking the energy spectrum of the decomposed wavelet signals of dynamic responses as the inputs of the NN can simplify the NN design for structural damage detection and it possesses a high sensitivity to small damage. Experimental results also show that the NN designed in this study can accurately detect multiple damage parameters or give some significant reference range of the damage parameters.

1. Introduction

Inputs and outputs of an artificial neural network (ANN) can form some nonlinear mapping between two state spaces. In particular, a typical supervised feed-forward back propagation (BP) ANN with hidden layers and sigmoid activation functions can approximate any smooth mapping. Such characteristics of ANN have been widely applied to the identification and detection of engineering structural damage [1–3]. As is known, the mapping relation of the ANN between the abstract features (e.g. the natural frequency, modal energy and transform function of structural vibration) and the physical parameters (e.g. structural damage parameters, such as crack locations and magnitudes) is obtained by sample training of the ANN. The integrality and accuracy of the mapping relationship between the two state spaces is the key factor for an accurate identification and detection of structural damage status. This depends on the training precision, the number of training samples and the number of inputs and outputs, as well as the design of the hidden layer of the ANN, etc. Besides, the selection of a structural damage index as the inputs of ANN and the indicative ability of the damage index for practical damage are also essential factors for the successful detection and identification of structural damage using the designed ANN.

The mechanical damage in a structure will cause some variation of structural dynamic characteristics, and various structural vibration parameters have been used as the input of the ANN in structural damage identification. The dynamic response of a servicing structure can be easily measured using a piezoelectric smart structure technique [4], which is technically simple, economical and feasible in practical engineering. Much published literature has shown the feasibility of this method in structural damage detection. Tsou and Shen [5] presented a method of on-line damage identification for two spring–mass systems. The damage characteristics (location and severity) of the system were detected and identified from the change of its dynamic properties (eigenvalues and mode shapes) through a BP neural network (NN). Stavroulakis and Antes [6] showed an inverse crack identification problem in linear elastodynamics using harmonic excitation, BP NN methods and boundary element techniques. The existence and characteristics of a hidden crack within an elastic structure were determined by means of measurements of the structural response at the accessible boundary for given external time-periodic loadings. Chang *et al* [7] proposed a structural damage detection method based

[3] Author to whom any correspondence should be addressed.

on parameter identification using an iterative NN technique for a clamped–clamped T beam. The structural parameters were assumed with different levels of reduction to simulate various degrees of structural damage. The trained NN model is used to predict the structural parameters by feeding in measured structural dynamic characteristics.

However, the structural model and damage status in the previous research are often simple and idealized, and only a few output categories of the ANN are considered. Thus, the acquired results may be inapplicable for the identification and detection of complex damage status of practical engineering structures. Because the final purpose of the theoretical research is its practical application, it is necessary to select a research model close to the application background of practical engineering. In this study, a honeycomb sandwich plate similar to practical engineering structures is taken as the study model for structural damage detection using ANN. Honeycomb sandwich composite plates have been widely applied to aeronautical structures as well as building, automobile and train structures, because it possesses many advantages, such as lighter weight, higher stiffness, heat insulation and preservation, and anti-radiation. Usually, this kind of structural material is made of very thin aluminum alloy, FRP (fiberglass-reinforced plastics), PVC and CERBP (ceramic fiber round braided rope), etc. One of its excellent properties is its light weight, typically only 10–15% of that of a solid structure using the same material. However, the ability to resist impact of a honeycomb sandwich plate is very poor, so crack and delamination damage occurs frequently. This will seriously affect the function of the structural components, such as the propeller of a helicopter, an aerofoil and a sealed cabin. Obviously, the study of in-service damage detection for honeycomb sandwich structures possesses significant application values.

Although structural dynamic response data can be applied to ANN for damage detection, a very serious obstacle exists: the amount of dynamic response data, which is determined by the number of spatial response locations and the number of spectral lines, is too large for the neural network to solve engineering problems. The direct use of such data will lead to a very large number of input nodes of the NN, which will in turn require a very large number of connections. Such networks are impractical in both training effort and convergence stability. In order to avoid large NNs, the energy spectrum of the structural dynamic response decomposed by wavelet transform is used to establish the input state space of the ANN. Wavelet analysis of a time-varying signal is a kind of localization analysis method in time and frequency domains, and the signal processing method has higher frequency and time resolution because its time and frequency windows can both be changed [8]. Researchers [9, 10] have shown that the energy spectrum of the structural dynamic response decomposed by wavelet transform has a high sensitivity to small structural damage. Generally, it is enough to select several tens (10–50) of orders of the energy spectrum for damage detection, i.e. only several tens of ANN inputs are needed. Therefore, this approach cannot only reduce the size of the ANN, but also detect small structural damage.

Although taking the energy spectrum of the decomposed wavelet signals of the structural dynamic response as the inputs of the ANN can decrease the required number of inputs and training samples, whether the trained ANN can accurately indicate the complex damage status in engineering practice still needs further discussion. Because there is no universal rule for the determination of the nodal number of an ANN hidden layer, how to select the number of training samples so as to optimize the performance of the designed ANN will depend on the case to be analyzed. Only a little literature is found to be relevant to the determination of training sample number, nodal number of the hidden layer and the training precision of the ANN. Zang and Imregun [11] suggested a design criterion $s = 1 + h(n + m + 1)/m$ for the number of training samples, where s is the number of training samples, n is the nodal number of the input layer, m is the nodal number of the output layer and h is the nodal number of the hidden layer. However, Weigend *et al* [12] pointed out that the criterion should be $1.1s/10 \leqslant h(n + 1) < 3s/10$. The difference between these two criteria is obvious.

This study presents a method for the detection of locations and extents of crack damage in honeycomb sandwich plates using both numerical simulations and experiments. Based on structural dynamic responses, wavelet transform is used for enhancing damage identification precision and compressing the total amount of input data. Back-propagation artificial neural networks (BP ANN) are used for classifying and identifying structural crack damage.

2. Dynamic model and responses of a honeycomb sandwich plate with crack damage

When the ANN is trained for establishing a mapping relationship between structural damage parameters (such as crack length, crack number, etc) and damage feature proxy (energy spectrum of the structural dynamic response decomposed using wavelet transform), a large number of sample data of the damage feature proxy and damage parameters are necessary. If all of these sample data are acquired only by experiment, it is too costly and inadvisable. The finite element dynamics model of damaged structures can be used to produce these sample data. Then, the ability of the trained ANN to identify structural damage can be verified using a small quantity of experimental sample data. Therefore, the finite element dynamics model of a honeycomb sandwich plate with crack damage is first established for acquiring the data of the structural vibration response. Then the feature proxy of structural damage can be extracted from these response signals.

When a crack exists in a honeycomb sandwich plate, it can be described using five parameters: depth d, length l, directional angle α and location coordinates x_c and y_c. Assuming that only a very narrow crack is considered, the crack width can be approximately taken as zero. A crack damage status can be expressed as

$$g = g(x_c, y_c, l, d, \alpha). \tag{1}$$

A model of the honeycomb sandwich plate with crack damage is shown in figure 1(a) and the finite element grids are shown in figures 1(b) and (c). In this model, the dimensional changes of crack damage are expressed using different mesh divisions for the surface plates and the sandwich plate. In order to condense the contents of this paper, the detailed procedures for establishing the finite element model is omitted (see [13]).

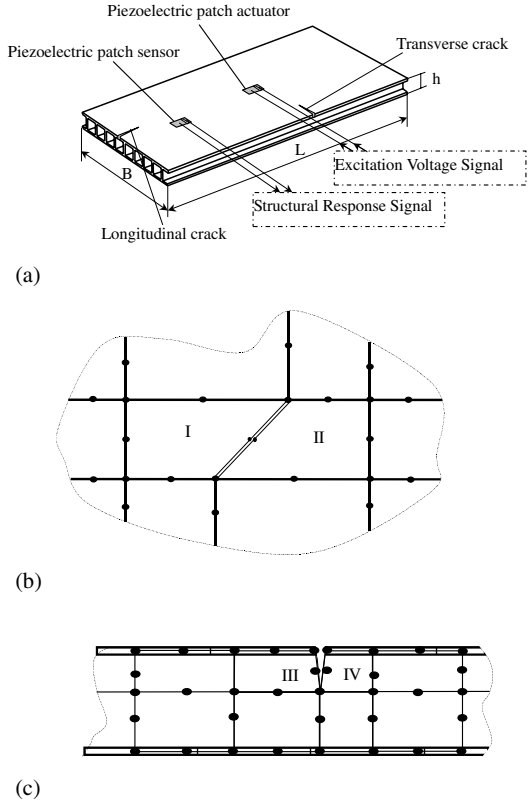

Figure 1. Crack damage in a honeycomb sandwich plate. (a) Model and vibration response measurement of a honeycomb plate with crack, (b) FEM grid division in the surface plate for indicating crack damage and (c) FEM grid division in stiffened plate for indicating crack damage.

The equation of motion of the composite plate with crack damage can be written as

$$\boldsymbol{M}\ddot{\Delta}(t) + \boldsymbol{C}(g)\dot{\Delta}(t) + \boldsymbol{K}(g)\Delta(t) = \boldsymbol{F}(t) \tag{2}$$

where $\boldsymbol{M}$, $\boldsymbol{K}(g)$ and $\boldsymbol{C}(g)$ are the global mass, damping and stiffness matrices of the structure, respectively, and $\boldsymbol{F}(t)$ is the external force vector. $\ddot{\Delta}$, $\dot{\Delta}$ and Δ are the global nodal acceleration, velocity and displacement vectors, respectively. In equation (2), the influence of crack damage on the mass matrix is ignored because the mass matrix rarely varies with crack status.

Because it is very difficult to determine the damping of materials and structures using calculation, many hypotheses are often adopted in establishing a structural dynamics model. One of the most commonly used hypotheses is the proportional damping, i.e. $\boldsymbol{C} = \beta_1\boldsymbol{M} + \beta_2\boldsymbol{K}$, where $\boldsymbol{C}$, $\boldsymbol{M}$ and $\boldsymbol{K}$ are structural damping, mass and stiffness matrices, respectively. β_1 and β_2 are constant coefficients. The determination of β_1 and β_2 was reported in many papers based on various hypotheses. Here, a method for determining the proportional damping based on modal transform is presented. Let Φ be the normalized modal matrix of structural vibration. Then the damping matrix $\boldsymbol{C}$ can be transformed as

$$\Phi^{\mathrm{T}}\boldsymbol{C}\Phi = \Phi^{\mathrm{T}}(\beta_1\boldsymbol{M} + \beta_2\boldsymbol{K})\Phi \Rightarrow 2\zeta_i\omega_i = \beta_1 + \beta_2\omega_i^2 \quad (i = 1, 2, \ldots, n) \tag{3a}$$

where ω_i and ζ_i are the ith natural frequency and modal damping ratio, respectively. Obviously, if ω_i and ζ_i are known, β_1 and β_2 could be determined. In practice, ω_i can be easily acquired using experiment or model simulation, but ζ_i is generally obtained only using experimental modal analysis. The ζ_i mainly depends on material properties. Generally, $\zeta_i = 0.1$–1% for most steel products and $\zeta_i = 0.5$–5% for fiber composite materials. Since using experimental modal analysis to determine ζ_i is time consuming and not accurate, a simple method is to assume that $\zeta_1 = \zeta_2 = \cdots = \zeta$, and ζ is selected based on the structural materials. In this paper, ζ is selected as 0.8%. Using the experimentally measured 10 natural frequencies (see table 1) and $\zeta = 0.8\%$, one can obtain a set of simultaneous equations

$$\begin{aligned} \beta_1 + \beta_2\omega_1^2 &= 2\zeta\omega_1 \\ \beta_1 + \beta_2\omega_2^2 &= 2\zeta\omega_2 \\ &\cdots\cdots\cdots\cdots \\ \beta_1 + \beta_2\omega_{10}^2 &= 2\zeta\omega_{10}. \end{aligned} \tag{3b}$$

Using the least square method to solve equation (3b) gives

$$\begin{bmatrix} \sum_{i=1}^{10} 1 & \sum_{i=1}^{10} \omega_i^2 \\ \sum_{i=1}^{10} \omega_i^2 & \sum_{i=1}^{10} (\omega_i^2)_2 \end{bmatrix} \begin{Bmatrix} \beta_1 \\ \beta_2 \end{Bmatrix} = \begin{Bmatrix} \sum_{i=1}^{10} 2\zeta\omega_i \\ \sum_{i=1}^{10} (\omega_i^2 \times 2\zeta\omega_i) \end{Bmatrix}. \tag{4}$$

Substituting the known 10 ω_i and $\zeta = 0.8\%$ into equation (4) yields $\beta_1 = 1.005\,777\,91$ and $\beta_2 = 0.000\,047\,79 \Rightarrow \beta_1 + \beta_2 \approx 1$. It must be pointed out that this is only valid for a limited range of ζ values. On the other hand, since $\beta_1\boldsymbol{M}$ and $\beta_2\boldsymbol{K}$ have the same units, β_1 and β_2 should have different units, then $\beta_1 + \beta_2 = 1$ may not be valid for all engineering materials.

Three specimens of the above-mentioned numerical model with dimensions of length $L = 295$ mm, width $B = 98$ mm and thickness $h = 8$ mm are manufactured. These honeycomb sandwich plates are composed of PVC materials, and the top surface has a thin layer of aluminum coating. The plate weight is only 12.67% of a solid structure with the same dimensions and material. The PVC material parameters are $E = 3.5$ GPa, $\mu = 0.34$ and $\rho = 1.36$ kg m^{-3}.

The natural frequencies of an undamaged specimen of honeycomb sandwich plate are experimentally measured to verify the reliability of the theoretical formula and the programs. The veracity and reliability of the established FEM structural dynamics model are verified using the experimentally measured natural frequencies for the intact structure only. The variations of structural natural frequencies and mode shapes due to small damage are not obvious, and

Table 1. Natural frequencies of the intact honeycomb sandwich plate obtained by experiment and numerical simulation.

Order	Numerical (Hz)	Experiment (Hz)	Errors (%)
1	29.711	28.5	4.2
2	50.900	52.5	3.0
3	80.826	82	1.4
4	106.99	108	1.0
5	139.70	134	4.2
6	162.70	158.5	2.6
7	192.16	184	4.4
8	212.43	208	2.1
9	250.42	261.5	4.2
10	277.07	287.5	3.6

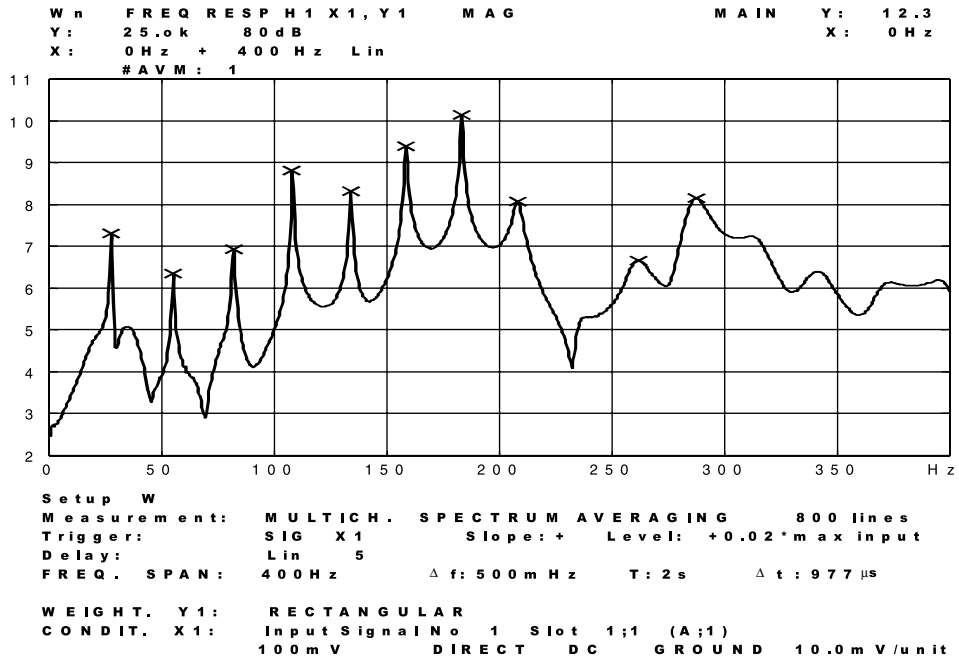

Figure 2. Experimental frequency response curve of the specimen.

they are quite difficult to detect using experimental methods. However, if the vibration responses for damaged structures are experimentally measured and the structural damage features are extracted based on wavelet transform, it is possible to detect small damage of structures. An experimentally obtained frequency response curve is given in figure 2. The lowest 10 features are extracted based on wavelet transform. The natural frequencies acquired by experiment and numerical simulation as well as the percentage errors between these two kinds of results are listed in table 1, which shows that the errors are below 5%. This is an acceptable numerical precision for engineering problems.

3. Construction of crack damage index vector based on wavelet transform

3.1. Wavelet transform

The traditionally used Fourier analysis is a kind of collectivity transform, i.e. either in time domain or in frequency domain, so it cannot synchronously express the local features of a signal in both time and frequency domains. However, this kind of feature is often the most pivotal in complex signal processing.

Wavelet transform possesses features of multi-resolution analysis and can express the local features of a signal in both time and frequency domains, i.e. its time window and frequency window can both be changed. Generally, wavelet transform possesses higher frequency resolution in the low frequency range for a signal, but it possesses higher time resolution in the high frequency range. These special characteristics are very useful for detecting transient or abnormal phenomena mixed in with normal signals, and it is also useful to exhibit the detailed components of such an abnormality. There are many published papers on wavelet analysis theory and its application in different fields [14]. It is shown that wavelet analysis is more powerful than traditional Fourier analysis in vibration-based structural damage detection.

3.2. Vector of crack damage index

Vibration responses at a few spots of an in-service structure can be easily measured using the technology of piezoelectric smart structures. However, the raw response signal cannot be used directly to identify structural damage quantitatively. Some representative indexes have to be selected and constructed.

A comparison of the energy of dynamic responses between cracked and intact structures in some special frequency bands exhibits some remarkable differences. This is because structural damage will suppress or enhance certain components of the response signals in some special frequency bands, i.e. structural damage can cause an energy increase of some response signal components or an energy decrease of some other response signal components. Therefore, the energy of structural vibration signals with different frequency components contains ample information on structural damage and the energy variation of one or several frequency components of the signals can indicate a special status of structural damage.

In order to extract structural damage information from structural response signals, the signal is first decomposed into multiple sub-signals in various frequency bands using WPA. Let $S_{0,0}(t)$ denote the original signal of the structural response, which can be expressed as

$$S_{0,0}(t) = \sum_{j=1}^{2^{k-1}} S_{k,j}(t) \tag{5}$$

where $S_{k,j}(t)$ is the sub-signal with orthogonal frequency band and k indicates the layer number of the tree structure of wavelet decomposition. The energy of the jth order sub-signals can

be expressed as

$$U_{k,j} = \int |S_{k,j}(t)|^2 \, \mathrm{d}t. \tag{6}$$

Assuming that the energy of the jth-order sub-signals of the intact and damaged structures are $U^0_{k,j}$ and $U^{\mathrm{d}}_{k,j}$, respectively, a non-dimensional index vector can be composed as follows:

$$\begin{aligned} V_{\mathrm{d}} &= \{v_1, v_2, \ldots, v_{2^{k-1}}\}^{\mathrm{T}} \\ &= \left\{1 - \frac{U^{\mathrm{d}}_{k,1}}{U^0_{k,1}}, 1 - \frac{U^{\mathrm{d}}_{k,2}}{U^0_{k,2}}, \ldots, 1 - \frac{U^{\mathrm{d}}_{k,2^{k-1}}}{U^0_{k,2^{k-1}}}\right\}^{\mathrm{T}}. \end{aligned} \tag{7}$$

Obviously, the element magnitudes of different index vectors V_{d} not only indicate the differences between the intact and damaged structures, but also imply the changes of different structural damage status.

4. Crack damage identification using neural networks

4.1. Neural networks and classifier

ANNs could provide a general, non-linear parameterized mapping between a set of inputs and outputs. A three-layer network with sigmoid activation functions can approximate any smooth mapping and it will be used here. A typical supervised feed-forward multi-layer NN is referred to as a BP NN. The network consists of three types of layers:

(1) the input layer that receives the structural damage index data;
(2) the hidden layer, which processes the data; and
(3) the output layer, that indicates the structural crack damage status.

The ability of identifying the structural crack damage status is acquired through neural network training using the known samples by the generalized delta learning algorithm. For a NN with n input nodes, m output nodes and N known training samples, the learning algorithm is designed to minimize recursively an error function E_{r} of the form

$$E_N = \sqrt{\frac{1}{N}\sum_{i=1}^{N}\sum_{j=1}^{m}(y_{ij} - d_{ij})^2}, \tag{8}$$

where y_{ij} and d_{ij} are the desired output (target) and the actual output values at the jth output node of the ith training sample, respectively. Let the input and output vectors of the NN be denoted by $x = \{x_1, x_2, \ldots, x_n\}^{\mathrm{T}}$ and $d = \{d_1, d_2, \ldots, d_m\}^{\mathrm{T}}$, respectively. The corresponding target output vector is $y = \{y_1, y_2, \ldots, y_m\}$, and $\{w_{kl}\}^p$ is the weight function between the input node k and the output node l at the pth layer. A non-linear sigmoid function f can be defined as

$$f(x) = \frac{1}{1 + \mathrm{e}^{-x}}. \tag{9}$$

The output of the kth node in the hidden and output layers can be described by

$$d_l = f(\mathrm{net}_l) = f\left(\sum_{k=1} w_{kl} d_k\right) \tag{10}$$

where net_l is the input of the kth node.

The interconnection weights, adjusted in such a way that the prediction errors on the training set can be minimized, are given by

$$\Delta_N w_{ji} = \beta \delta_{Nj} d_{Ni} \tag{11}$$

where $0 < \beta < 1$ is the learning rate coefficient, Δ is the actual change in the weight and δ is the error at the node, which can be expressed as

$$\delta_{Nj} = (y_{Nj} - d_{Nj})(1 - d_{Nj})d_{Nj}$$
(if node j is in the output layer) (12)

$$\delta_{Nj} = d_{Nj}(1 - d_{Nj}) \sum_i \delta_{Ni} w_{ij}$$
(if node j is in the hidden layer). (13)

In order to control the network oscillations during the training process, a momentum coefficient $0 < \alpha < 1$ is introduced to the definition of the weight change:

$$\Delta_N w_{ji}(t+1) = \beta \delta_{Nj} d_{Nj} + \alpha \Delta_N w_{ji}(t). \tag{14}$$

Once the change is computed, the new weight is given by

$$w_{ji}(t+1) = w_{ji}(t) + \Delta_N w_{ji}(t+1). \tag{15}$$

The training of a BP NN is a two-step procedure. In the first stage, the network propagates an input through each layer until an output is generated. The error between the actual output d_{Ni} and the target output y_{Ni} is then computed using equation (8). In the second stage, the calculated error is transmitted backwards from the output layer and the weights are adjusted according to equations (14) and (15) in order to minimize the error. The training process is terminated when the error E_{r} is sufficiently small for all training samples.

4.2. Implementation of neural network algorithm

As mentioned earlier, a sample of structural dynamic responses with 2048 sample data can be expressed using an index vector with 32 elements, which are composed of the energy spectrum of structural dynamic responses decomposed using wavelet transform. Thus, the nodal number of the input layer can be determined as $n = 32$. If the structural dynamic responses are directly used as the input to the NN, 2048 input nodes are needed. Obviously, the currently required nodal number in the input layer is greatly reduced because of the data compression ability of wavelet transform. The training data are extracted from numerical simulation of a structural dynamics model. A large number of sample data are required in NN training, and it is costly and time-consuming if these data were acquired by experiment only. In this paper, the structural dynamics model is verified using experimental measurement of structural natural frequencies and vibration responses to excitation.

The node number of the output layer m depends on the pre-selected crack damage status. In this study for crack detection of a honeycomb sandwich plate, the following crack damage statuses are considered:

(1) crack direction of 0° or 90° (longitudinal or transverse crack) is expressed using one binary nodal output (0 or 1);
(2) the three kinds of crack depth (5%h, 10%h and 15%h) are denoted using the nodal outputs with two digits (10, 01, and 11);

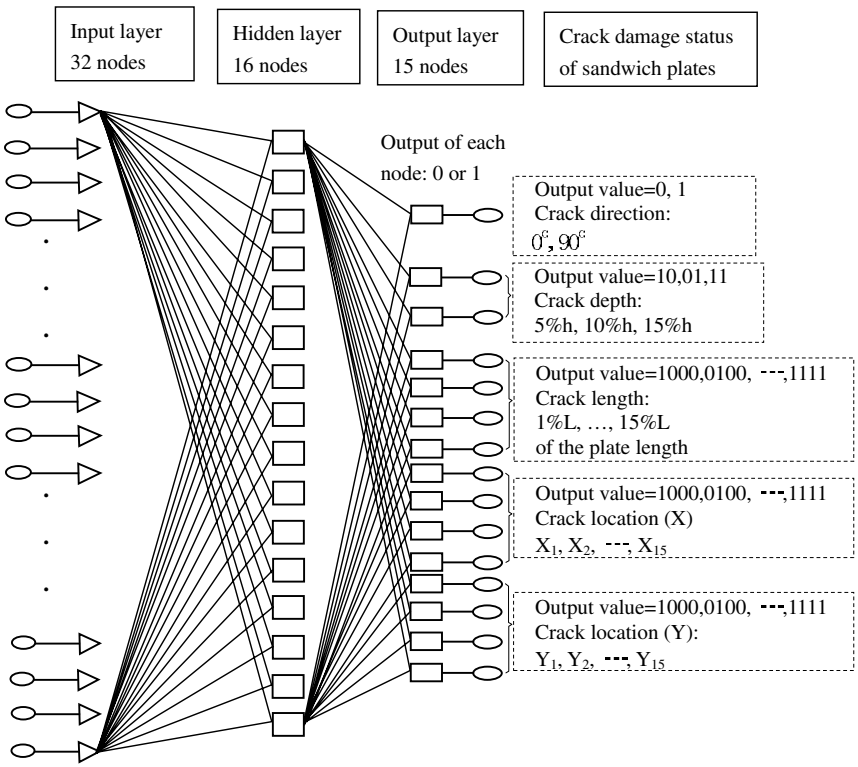

Figure 3. Back propagation neural network for identification of multiple crack parameters.

(3) the 15 kinds of crack length ($1\%L$, $2\%L$, $3\%L$, $4\%L$, ..., $15\%L$) are represented using the nodal outputs with four digits (1000, 0100, 1100, 0010, ..., 1111);
(4) the 15 kinds of x and 15 kinds of y coordinates of the crack location, i.e. X_1–X_{15} = 5, 15, 25, 30, 35, 40, 45, 50, 55, 60, 65, 70, 75, 85, 95% of plate length L, and Y_1–Y_{15} = 5, 15, 25, 30, 35, 40, 45, 50, 55, 60, 65, 70, 75, 85, 95% of plate width B, are described using two sets of nodal outputs with four digits (1000, 0100, 1100, 0010, ..., 1111), respectively (see figure 3).

Thus, there are altogether 15 nodes in the output layer of this NN. Because the maximum decimal value of the 15 binary nodes is $2^{15}-1 = 32\,767$, the output layer can represent 32 767 kinds of crack damage status. The case without damage will be indicated using the value 0 at all 15 nodes in the output layer.

The nodal number of the hidden layer h is generally selected as half of that of the input layer, i.e. $h = n/2 = 16$ [11]. This BP network is shown in figure 3. The relationship among the number of training samples N, the number of input variable n, the number of output variables m and the number of hidden layer nodes h can be approximately expressed as [15]

$$N = 1 + h(n + m + 1)/m. \tag{16}$$

In this study, $n = 32$, $m = 15$ and $h = 16$, then the required number of training samples N should equal 53, which is a reasonable number of training samples for experiment and numerical simulation. Equation (16) shows that the number of required training samples increases with that of input variables. If the number of input variables is much larger than the number of training samples, the NNs will focus on local details of individual training samples, which may be meaningless in a global context. On the other hand, equation (16) also implies that the larger the number of output variables, the smaller the number of required training samples will be. However, more output variables will take a longer time for the training of neural networks and the performance of the NN may be reduced.

Generally, better training results for NNs will be obtained if more training samples are used. However, the required workload for acquiring training data is an important issue. Although using numerical simulation to acquire the training data may be easier than using experiments, it is very time-consuming for numerical analysis on complex structures if a large number of training data are required. How to reduce the number of training samples while still keeping the training effect is a very important issue in the design of NNs. So far, there have been various methods for determining the number of training samples and this number will depend on the final effect of NN training.

4.3. Neural network training and verification

All combinations of the above-mentioned crack damage and undamaged status will produce $2^{15} = 32\,768$ cases. Using all these cases as samples for NN training is neither necessary nor possible for practical implementation, even if numerical simulation is used. According to equation (16), 60 samples of the damaged structures and one sample of the intact structure are selected for training and verification of this NN. The cases of crack damage of these 60 samples are shown in figure 4 and their output codes are listed in table 2. Obviously, each input sample corresponds to one output string code with 15 bits

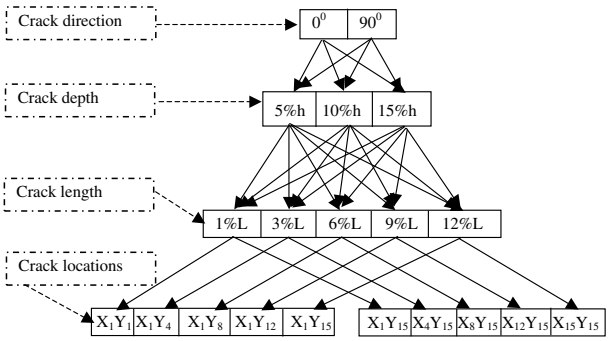

Figure 4. Crack damage status of 60 samples for training and simulation of the ANN.

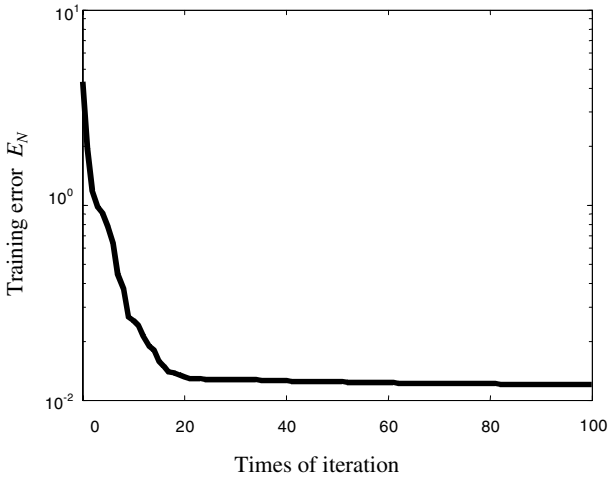

Figure 5. Training errors for the designed neural network.

binary. The 1st–55th samples of the damaged structures and one sample of the intact structure are used for ANN training, and the 56–60th samples of the damaged structures are used for verification.

In fact, to select a set of widely representative train sample data will be very profitable for reducing the number of required training data and enhancing the efficiency of neural network training. Many complex special methods have been studied in this field. Since this paper mainly focuses on research into the integrated application of various methods of structural damage detection, the study into ways of selecting training samples was not emphasized here.

The training error versus times of iterations is plotted in figure 5. As can be seen from figure 5, the training error decreases with times of iteration and satisfies the given criterion 0.02 after about 80 iterations. The anticipated outputs and the real outputs of this trained NN for the five verification samples are listed in table 3. The data in table 3 show that the maximum error between the anticipated and real output values is about 15%. This error level is acceptable, since the anticipated output is either 0 or 1, and it also indicates that the network is well trained and stable.

It is worth pointing out that, after an ANN is trained using the real-valued inputs and the binary type outputs, the outputs corresponding to the inputs which are used for the training data must be binary values. However, if a set of inputs, which does not belong to the training input data, is fed into the trained

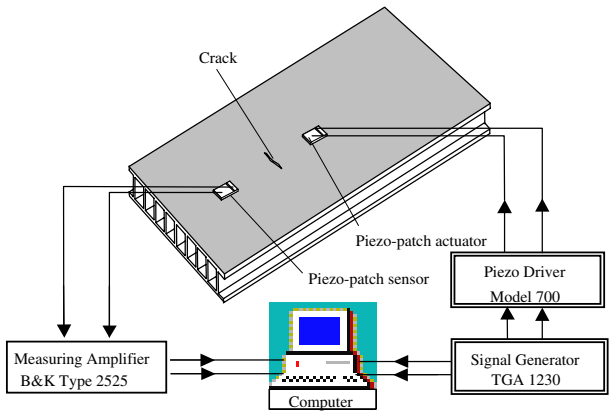

Figure 6. Schematic diagram of the experimental set-up for crack damage detection.
(This figure is in colour only in the electronic version)

ANN, the corresponding outputs are not always the binary values. Generally, the better the NN is trained, the closer to the binary values the output values will be. Since all initial link weights are randomly and automatically selected based on the range of input values to be used, these link weight values must be real values, so that the initial outputs are also real values. With the progress of training, the outputs will gradually converge to either 0 or 1. The advantage of taking binary as output is that this will make it easier to distinguish true or false output results in a large range of allowable error.

5. Structural dynamic testing and crack damage identification

In order to acquire the dynamic responses of the honeycomb sandwich plate, two piezo-patches with a dimension of 25 mm × 10 mm × 0.28 mm are bonded on the surface of the plate. A square wave signal with 150 mV magnitude and 5 Hz frequency generated by the signal generator TGA 1230 is fed into the TRek Model 700 Piezo-driver. The 30 V voltage signal from the output of the Piezo-driver is exerted on the piezo-patch actuator. The dynamic responses of the plate are measured by the piezo-patch sensor and they are first fed into the B&K 2525 measuring amplifier, which can amplify the signal and filter out the noise using the 3–3 kHz band-pass function. Then, the output signal from the measuring amplifier is taken as the input to a computer with an A/D card for data sampling and storage. The experimental set-up for acquisition of the dynamic responses of the plate with different crack lengths is shown in figure 6. The measured excitation signal and the dynamic response signals for the intact and damaged honeycomb sandwich plates are shown in figure 7. An example of raw time signals of the plate dynamic response and its wavelet decomposition is shown in figure 8. One can see that it is difficult to make a quantitative analysis for plate damage detection using the time domain dynamic response or the decomposed wavelet signals. However, the energy spectrum established according to equation (7) can show more detailed information. Figure 9 shows the energy spectrum distribution of the dynamic response decomposed by wavelet transform for three plate specimens, which contain a crack with

Table 2. Known binary output codes with 15 bits of 55 train and 5 verification samples.

Crack status	α	d		l				X_i				Y_i			
Output bit	1	2	3	4	5	6	7	8	9	10	11	12	13	14	15
Case 1	0	1	0	1	0	0	0	1	0	0	0	1	0	0	0
Case 2	0	1	0	1	1	0	0	1	0	0	0	0	0	1	0
Case 3	0	1	0	0	1	1	0	1	0	0	0	0	0	0	1
Case 4	0	1	0	1	0	0	1	1	0	0	0	0	0	1	1
Case 5	0	1	0	0	0	1	1	1	0	0	0	1	1	1	1
Case 6	0	1	0	1	0	0	0	1	0	0	0	1	1	1	1
Case 7	0	1	0	1	1	0	0	0	0	1	0	1	1	1	1
Case 8	0	1	0	0	1	1	0	0	0	0	1	1	1	1	1
Case 9	0	1	0	1	0	0	1	0	0	1	1	1	1	1	1
Case 10	0	1	0	0	0	1	1	1	1	1	1	1	1	1	1
Case 11	0	0	1	1	0	0	0	1	0	0	0	1	0	0	0
Case 12	0	0	1	1	1	0	0	1	0	0	0	0	0	1	0
Case 13	0	0	1	0	1	1	0	1	0	0	0	0	0	0	1
Case 14	0	0	1	1	0	0	1	1	0	0	0	0	0	1	1
Case 15	0	0	1	0	0	1	1	1	0	0	0	1	1	1	1
Case 16	0	0	1	1	0	0	0	1	0	0	0	1	1	1	1
Case 17	0	0	1	1	1	0	0	0	0	1	0	1	1	1	1
Case 18	0	0	1	0	1	1	0	0	0	0	1	1	1	1	1
Case 19	0	0	1	1	0	0	1	0	0	1	1	1	1	1	1
Case 20	0	0	1	0	0	1	1	1	1	1	1	1	1	1	1
Case 21	0	1	1	1	0	0	0	1	0	0	0	1	0	0	0
Case 22	0	1	1	1	1	0	0	1	0	0	0	0	0	1	0
Case 23	0	1	1	0	1	1	0	1	0	0	0	0	0	0	1
Case 24	0	1	1	1	0	0	1	1	0	0	0	0	0	1	1
Case 25	0	1	1	0	0	1	1	1	0	0	0	1	1	1	1
Case 26	0	1	1	1	0	0	0	1	0	0	0	1	1	1	1
Case 27	0	1	1	1	1	0	0	0	0	1	0	1	1	1	1
Case 28	0	1	1	0	1	1	0	0	0	0	1	1	1	1	1
Case 29	0	1	1	1	0	0	1	0	0	1	1	1	1	1	1
Case 30	0	1	1	0	0	1	1	1	1	1	1	1	1	1	1
Case 31	1	1	0	1	0	0	0	1	0	0	0	1	0	0	0
Case 32	1	1	0	1	1	0	0	1	0	0	0	0	0	1	0
Case 33	1	1	0	0	1	1	0	1	0	0	0	0	0	0	1
Case 34	1	1	0	1	0	0	1	1	0	0	0	0	0	1	1
Case 35	1	1	0	0	0	1	1	1	0	0	0	1	1	1	1
Case 36	1	1	0	1	0	0	0	1	0	0	0	1	1	1	1
Case 37	1	1	0	1	1	0	0	0	0	1	0	1	1	1	1
Case 38	1	1	0	0	1	1	0	0	0	0	1	1	1	1	1
Case 39	1	1	0	1	0	0	1	0	0	1	1	1	1	1	1
Case 40	1	1	0	0	0	1	1	1	1	1	1	1	1	1	1
Case 41	1	0	1	1	0	0	0	1	0	0	0	1	0	0	0
Case 42	1	0	1	1	1	0	0	1	0	0	0	0	0	1	0
Case 43	1	0	1	0	1	1	0	1	0	0	0	0	0	0	1
Case 44	1	0	1	1	0	0	1	1	0	0	0	0	0	1	1
Case 45	1	0	1	0	0	1	1	1	0	0	0	1	1	1	1
Case 46	1	0	1	1	0	0	0	1	0	0	0	1	1	1	1
Case 47	1	0	1	1	1	0	0	0	0	1	0	1	1	1	1
Case 48	1	0	1	0	1	1	0	0	0	0	1	1	1	1	1
Case 49	1	0	1	1	0	0	1	0	0	1	1	1	1	1	1
Case 50	1	0	1	0	0	1	1	1	1	1	1	1	1	1	1
Case 51	1	1	1	1	0	0	0	1	0	0	0	1	0	0	0
Case 52	1	1	1	1	1	0	0	1	0	0	0	0	0	1	0
Case 53	1	1	1	0	1	1	0	1	0	0	0	0	0	0	1
Case 54	1	1	1	1	0	0	1	1	0	0	0	0	0	1	1
Case 55	1	1	1	0	0	1	1	1	0	0	0	1	1	1	1
Case 56	**1**	**1**	**1**	**1**	**0**	**0**	**0**	**1**	**0**	**0**	**0**	**1**	**1**	**1**	**1**
Case 57	**1**	**1**	**1**	**1**	**1**	**0**	**0**	**0**	**0**	**1**	**0**	**1**	**1**	**1**	**1**
Case 58	**1**	**1**	**1**	**0**	**1**	**1**	**0**	**0**	**0**	**0**	**1**	**1**	**1**	**1**	**1**
Case 59	**1**	**1**	**1**	**1**	**0**	**0**	**1**	**0**	**0**	**1**	**1**	**1**	**1**	**1**	**1**
Case 60	**1**	**1**	**1**	**0**	**0**	**1**	**1**	**1**	**1**	**1**	**1**	**1**	**1**	**1**	**1**

a length of $3\%L$, $6\%L$ and $9\%L$, respectively. One can find that, among the element values of the damage index vector V_{d}, several element values exhibit the tendency to increase with the crack length, such as the 25th-order element. Obviously, the magnitudes and order number of the energy spectrum can quantitatively indicate a structural damage status.

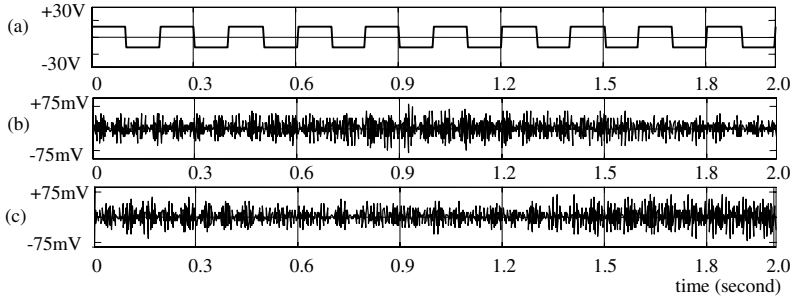

Figure 7. Excitation and dynamic responses of a plate specimen. (a) Excitation signal exerted on a piezoelectric patch actuator, (b) dynamic response from a piezoelectric patch sensor bonded on the intact plate, and (c) dynamic response from a piezoelectric patch sensor bonded on the plate with a crack.

Table 3. Anticipated outputs and real outputs of the trained NN for the five verification samples (AO = anticipated output; RO = real output).

Output bit	Case 56		Case 57		Case 58		Case 59		Case 60	
	AO	RO	AO	RO	AO	RO	AO	RO	AO	RO
1	1	0.9409	1	0.9071	1	1.1261	1	1.0516	1	1.1032
2	1	1.0674	1	1.0358	1	1.1476	1	1.0228	1	1.0746
3	1	1.1067	1	1.0081	1	1.0152	1	1.0593	1	1.0443
4	**1**	1.1463	**1**	1.1503	**0**	0.1970	**1**	0.8486	**0**	−0.1329
5	**0**	0.0510	**1**	1.0242	**1**	1.0162	**0**	0.0980	**0**	0.0562
6	**0**	0.1836	**0**	−0.0587	**1**	0.9968	**0**	0.0182	**1**	1.0181
7	**0**	0.1976	**0**	0.1960	**0**	0.0257	**1**	1.1028	**1**	1.0016
8	1	1.0846	0	0.0977	0	0.0000	0	0.0423	1	1.0000
9	0	0.0081	0	0.1903	0	0.0537	0	0.1927	1	1.0367
10	0	0.0436	1	1.0188	0	0.0267	1	1.0240	1	1.0185
11	0	0.1880	0	0.1012	1	0.7108	1	0.9538	1	1.1901
12	1	0.9773	1	1.0505	1	1.0393	1	1.0496	1	1.1096
13	1	0.9408	1	1.0953	1	1.1075	1	1.0819	1	1.0988
14	1	0.9574	1	1.0565	1	1.1623	1	0.9847	1	0.8683
15	1	1.0423	1	0.9784	1	1.0053	1	1.0143	1	1.0011

Table 4. Real outputs of the trained ANN and the theoretical outputs corresponding to practical damage for the three plate specimens. EP1–EP3: number of plate samples; RO: real outputs of the trained ANN; AO: approximate output values according to a maximum allowable error of 25%; TO: theoretic outputs and $*$ may be 0 or 1 (unable to be determined).

Crack status and output bit		EP1			EP2			EP3		
		RO	AO	TO	RO	AO	TO	RO	AO	TO
Direct. angle	1	1.24	1	1	1.22	1	1	−0.15	0	0
Crack depth	2	−0.28	0	0	0.06	0	0	0.06	0	0
	3	1.14	1	1	1.25	1	1	1.12	1	1
Crack length	4	1.20	1	1	0.16	0	0	1.06	1	1
	5	1.24	1	1	1.26	1	1	−0.17	0	0
	6	0.18	0	0	1.14	1	1	0.14	0	0
	7	0.33	$*$	0	0.19	0	0	0.89	1	1
Location in x direction	8	0.19	0	0	0.26	0	0	−0.16	0	0
	9	0.49	$*$	1	1.23	1	1	1.12	1	1
	10	0.76	#	0	0.20	0	0	0.12	0	0
	11	0.21	0	0	0.24	0	0	0.17	0	0
Location in y direction	12	0.19	0	0	1.10	1	1	1.10	1	1
	13	1.22	1	1	0.29	$*$	0	0.14	0	0
	14	0.59	$*$	0	0.78	1	1	0.16	0	0
	15	0.54	$*$	0	0.34	$*$	0	1.10	1	1

Finally, damage detection of three practical honeycomb sandwich plates is carried out. The crack damage of three plate specimens EP1, EP2 and EP3 are in turn as follows: crack direction = 90°, 90° and 0°; crack depth = $10\%h$, $10\%h$ and $10\%h$; crack length = $3\%L$, $6\%L$ and $9\%L$; the locations in x-coordinate = $15\%L(x_2)$, $15\%L(x_2)$ and $15\%L(x_2)$; the locations in y-coordinate = $15\%B(y_2)$, $35\%B(y_5)$ and $55\%B(y_9)$. According to figure 3, the three sets of theoretical output codes should be 101110001000100, 101011001001010 and 001100101001001, respectively. The

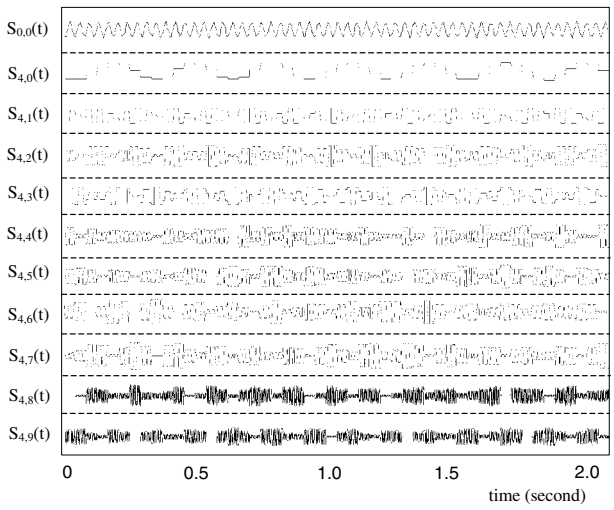

Figure 8. Raw time signals of dynamic responses and their wavelet decomposition.

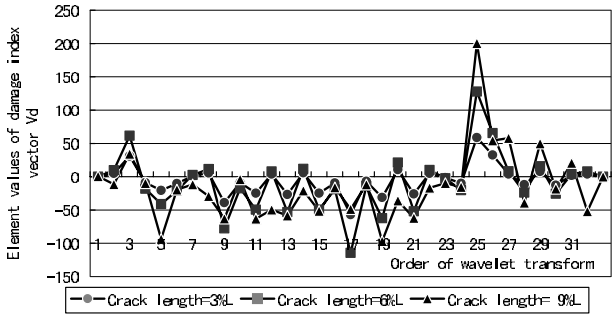

Figure 9. Element values of damage index vector V_d with different crack lengths.

dynamic responses of the three plate specimens are measured using the set-up shown in figure 6 and each set of the response data is decomposed into 32 orders of wavelet signals. The energy spectrum of the decomposed wavelet signals is calculated according to equation (7) and fed into the trained ANN. The actual outputs of the ANN and the theoretical outputs corresponding to the real damage status of these three plate specimens are listed in table 4.

In table 4, RO is the real output of the trained ANN, AO is the approximate output value according to a maximum allowable error of 25% and TO is the theoretical output. Here, AO is not the anticipated or theoretical output, it is obtained by transforming RO into an integer with the error limited to $\pm 25\%$. When the value of RO is in the range of $1 \pm 25\%$, it is transformed into 1; when the value of RO is in the range of $0 \pm 25\%$, it is transformed into 0; otherwise, the value of RO is taken as uncertain. Thus, the real number output can be converted into binary, so that the difference between RO and TO can be compared.

The output data of the ANN must be converted to 0 or 1 for the determination of crack damage status. Therefore, the real output data should be converted according to some error criterion. A maximum allowable error is set approximately as 25%, which is changeable according to the actual effect of damage detection. The converted values (AO) of the real outputs (RO) of cases EP1, EP2 and EP3 are also listed in table 4. From table 4 one can find that the results of cases EP2 and EP3 can accurately indicate the crack damage status of the plate specimens, and the average error of case EP3 is about 15%, but the average error of case EP2 is about 25%. In case EP1, because the errors of several output bits are too large to determine the value of AO as 0 or 1, some crack damage parameters cannot be confirmed. For instance, in case EP1 the errors of the 7th, 9th, 14th and 15th output bits almost reach 40–50%. Thus one cannot determine if they are 0 or 1 and there is an unmatched result for the 10th output bit. As a result, the crack length and location in x and y coordinates in case EP1 cannot be determined, because the crack length is too short.

After more prudent analysis, one can find that the output error of the ANN increases gradually from EP3 to EP1, and some data in EP1 are not available. This is because the crack damage severity (crack length) decreases gradually from EP3 to EP1 and this phenomenon indicates that the damage severity (crack length) is a key factor in damage detection using the ANN.

Although one cannot accurately confirm all damage parameters for very small structural damage using the method proposed in this study, we can still acquire some valuable information about the structural damage status. In this way, a possible range for some structural damage parameters can be determined and this can provide very important guidance to practical engineering problems.

6. Conclusions

Dynamic responses of an in-service structure can be conveniently acquired using piezoelectric smart structure technology. It is feasible for crack damage detection of a honeycomb sandwich plate using the energy spectrum of dynamic responses decomposed by wavelet transform and the artificial neural network to be done. Based on the experimental results of crack damage detection for three plate specimens, various issues of detecting small cracks using the method proposed in this study are discussed. Results show that, using the energy spectrum of structural dynamic responses decomposed using wavelet transform, the sensitivity of structural damage detection can be enhanced. In addition, the required number of inputs to the NN can be greatly reduced so as to reduce the time and effort needed for ANN training. Though for very small structural damage not all the damage parameters can be accurately determined using the method proposed in this study, a possible range of structural damage parameters can still be obtained and this has very important instructive value for practical engineering problems.

Acknowledgments

The work described in this paper has been supported by the Research Grants Council of Hong Kong Special Administrative Region, China (project no PolyU 5164/00E), and the Research Committee of the Hong Kong Polytechnic University (project no GT 621).

References

[1] Manning R A 1994 Structural damage detection using active members and neural networks *AIAA J.* **32** 1331–3

[2] Luo H and Hanagud S 1997 Dynamic learning rate neural network training and composite structural damage detection *AIAA J.* **35** 1522–7

[3] Yun C B and Bahng E Y 2000 Substructural identification using neural networks *Comput. Struct.* **77** 41–52

[4] Gobin P F, Jayet Y, Baboux J C, Salvia M, Chateauminois A, Abry J C and Giraud G 2000 New trends in non-destructive evaluation in relation to the smart materials concept *Int. J. Syst. Sci.* **31** 1351–9

[5] Tsou P Y and Shen M H H 1994 Structural damage detection and identification using neural networks *AIAA J.* **32** 176–83

[6] Stavroulakis G E and Antes H 1998 Neural crack identification in steady state elastodynamics *Comput. Methods Appl. Mech. Eng.* **165** 129–46

[7] Chang C C, Chang T Y P, Xu Y G and Wang M L 2000 Structural damage detection using an iterative neural network *J. Intell. Mater. Syst. Struct.* **11** 32–42

[8] Chui C K 1997 *Wavelets: A Mathematical Tool for Signal Processing* (Philadelphia, PA: Society for Industrial and Applied Mathematics)

[9] Yan Y J, Yam L H, Li Y Y and Wong W O 2001 Detection of crack damage in composite laminates usingsmart material and wavelet analysis *Proc. 8th Int. Congr. of Sound and Vibration (Hong Kong PolyU)* pp 2349–56

[10] Wang Q and Deng X M 1999 Damage detection with spatial wavelets *Int. J. Solids Struct.* **36** 3443–68

[11] Zang C and Imregun M 2001 Structural damage detection using artificial neural networks and measured FRF data reduced via principal component protection *J. Sound Vib.* **242** 813–27

[12] Weigend A S, Rumelhart D E and Huberman B A 1990 Predicting the future: a connections approach *Int. J. Neural Syst.* **1** 3

[13] Yam L H, Yan Y J, Li Y Y and Cheng L 2002 Feasibility of crack damage detection for a honeycomb sandwich plate using natural frequency and dynamic responses *Comput. Methods Appl. Mech. Eng.* submitted

[14] Jones C L, Lonergan G T and Mainwaring D E 1996 Wavelet packet computation of the Hurst exponent *J. Phys. A: Math. Gen.* **29** 2509–27

[15] Hasselman T K and Anderson M C 1998 Linking FEA and SEA by principal components analysis *Proc. 16th Int. Conf. on Modal Analysis (Santa Barbara, CA)* pp 1285–91